

EventGeM: Global-to-Local Feature Matching for Event-Based Visual Place Recognition

Adam D Hines^{1*} Gokul B Nair¹ Nicolás Marticorena¹ Michael Milford¹ Tobias Fischer¹

Abstract—Dynamic vision sensors, also known as event cameras, are rapidly rising in popularity for robotic and computer vision tasks due to their sparse activation and high-temporal resolution. Event cameras have been used in robotic navigation and localization tasks where accurate positioning needs to occur on small and frequent time scales, or when energy concerns are paramount. In this work, we present EventGeM, a state-of-the-art global to local feature fusion pipeline for event-based Visual Place Recognition. We use a pre-trained vision transformer (ViT-S/16) backbone to obtain global feature patch for initial match predictions embeddings from event histogram images. Local feature keypoints were then detected using a pre-trained MaxViT backbone for 2D-homography based re-ranking with RANSAC. For additional re-ranking refinement, we subsequently used a pre-trained vision foundation model for depth estimation to compare structural similarity between references and queries. Our work performs state-of-the-art localization when compared to the best currently available event-based place recognition method across several benchmark datasets and lighting conditions all whilst being fully capable of running in real-time when deployed across a variety of compute architectures. We demonstrate the capability of EventGeM in a real-world deployment on a robotic platform for online localization using event streams directly from an event camera. Project page: <https://eventgemvpr.github.io/>

I. INTRODUCTION

Visual place recognition (VPR) is a core component for robot localization and navigation, where incoming query images are matched to a known reference database [36]. State-of-the-art VPR systems use conventional frame-based images of places for feature extraction [43, 28]. Recently, there has been a growing interest in the use of dynamic vision sensors (DVS), also known as event-cameras, to perform VPR due to their low-power, low-latency operation and dense temporal information [8, 23, 9, 22, 24, 14, 33]. Existing methods to perform VPR using event frames including development with neuromorphic processors [14], event collection windows over long periods of time [9, 15], performing image reconstructions from event edges through deep-learned methods [24, 23], or complex fusion with RGB based VPR techniques [19]. By contrast, event-based VPR has not made use of or explored the use of any pre-trained deep learning systems that could be adapted for image retrieval [40, 41] in part, due to an absence of such models. Therefore, in this work we set out to create an

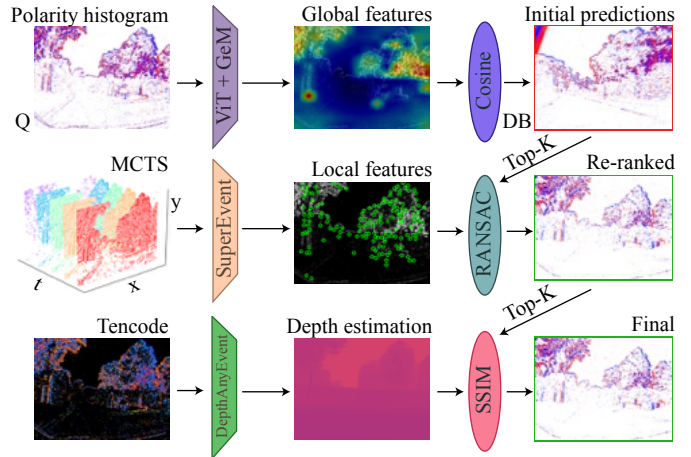


Fig. 1: Schematic overview of EventGeM. Polarity histogram frames are passed through a vision transformer [40] (ViT) and generalized mean pooling [32] (GeM) layer for global features and initial place predictions. Multi-channel time surface (MCTS) representations are passed through SuperEvent [6] for local feature detection and 2D-homography based re-ranking via RANSAC. An optional second re-ranking step uses tencode representations are used with Depth AnyEvent [2] to produce depth estimations for further refinement of matches using a structural similarity index metric (SSIM).

event-based VPR pipeline taking lessons and implementations from conventional systems [28], and demonstrate a significant improvement in VPR performance relative to existing baseline methods. To further demonstrate that event cameras are a valuable robotic vision sensor, we deploy our system on a navigating robot to perform real-time localization.

Whilst conventional VPR techniques using frame-based cameras benefit from a wide variety of pre-trained deep-learning models, such as from DINOv2 [31], ResNet [13], or VGG networks [37], event-based VPR methods are not directly compatible with such conventional computer vision models. This is because asynchronous event streams produce temporally rich, but sparse, information on microsecond timescales [11]. Simple representations of event frames, such as binary or histogram counts of pixel-wise event activity over a fixed time window, are among the most common ways of generating frames from asynchronous event camera streams for the purposes of computer vision applications [40, 41, 11, 15]. Recently, however, several vision backbones have been developed for event frames using student-teacher

¹These authors are with the QUT Centre for Robotics, School of Electrical Engineering and Robotics, Queensland University of Technology, Brisbane, QLD 4000, Australia. * Correspondence should be addressed to: adam.hines@qut.edu.au

This work received funding from an ARC Laureate Fellowship FL210100156 to MM and an ARC Discovery Early Career Researcher Award DE240100149 to TF. The authors acknowledge continued support from the Queensland University of Technology (QUT) through the Centre for Robotics.

paradigms with conventional RGB images to perform global feature detection [40, 41], keypoint detection [6], and depth estimation [2], demonstrating state-of-the-art performance.

In this work, we introduce a new event-based VPR pipeline called EventGeM that leverages these development in student-teacher refined ViTs. Specifically, we build upon the Event Camera Data Pre-Training (ECDPT) model which was originally designed for object detection and image segmentation [40]. To create compact global feature descriptors for VPR, we combine ECDPT with generalized mean pooling (GeM) [32] to perform initial place predictions using cosine distances for each query to all reference databases. We subsequently perform 2D-homography based re-ranking of top- k candidates with keypoint descriptors from SuperEvent, which uses a MaxViT backbone with a feature pyramid network and a grid-based visual geometry group (VGG) detector [6]. Finally, we optionally use depth maps from Depth AnyEvent [2], based on DINOv2, for 3D-geometry based match refinement (Fig. 1). Our method performs state-of-the-art VPR across several benchmark datasets and multiple conditions.

Importantly, we also demonstrate that EventGeM is a computationally efficient system that is capable of being run in real-time with high accuracy, relative to baseline methods that are either fast but inaccurate or accurate but computationally infeasible to be used in practice. To that end, we additionally showcase that EventGeM is capable of real-world deployment for online localization by demonstrating our method on a robotic platform running directly from a DVS. We are able to achieve an average runtime of 24 Hz per query with an accuracy of over 88% when operating online on an NVIDIA Jetson. This demonstrates with great potential of the capabilities an event driven system can have for practical applications in edge-deployed machines, robots, and autonomous systems.

Our contributions are as follows:

- Present EventGeM as the first event-based method to perform VPR with a vision transformer model and GeM pooling for global descriptor generation.
- Achieve state-of-the-art event-based localization performance by using, for the first time in an event-based pipeline, 2D-homography and 3D-geometry re-ranking using dual local feature keypoint and depth map structural similarity.
- Showcase real-time capable localization of our proposed system, including re-ranking, with an on-robot demonstration using an event-based camera.
- Fully open-source and provide an accessible system for future development available at <https://github.com/AdamDHines/Event-GeM>.

II. RELATED WORKS

In this section, we review conventional and state-of-the-art VPR systems in Section II-A, event-based localization and VPR methods in Section II-B, and deep-learning methods for event cameras that are used in navigation tasks in Section II-C.

A. Visual place recognition

VPR is an image retrieval task used in robotic navigation to match incoming query images to known reference database images [36]. Effective VPR methods need to be robust against severe visual changes, efficiently retrieve images, and prevent aliasing against similar looking places [28].

Modern VPR techniques have focused on employing state-of-the-art computer vision models, such vision foundation models (VFMs), to extract high quality features from images. SALAD [16] fine-tuned the DINOv2 VFM for optimal feature detection and introduced a new transport aggregation technique for global descriptors. MegaLoc [3] extended SALAD for any image retrieval task by combining multiple methods, training techniques, and datasets for a singular retrieval method to improve the robustness across different environments, while also improving per-query runtime. AnyLoc [20] similarly aimed to create a VPR pipeline for any environment, which extended to state-of-the-art performance in aerial imagery. MixVPR [1] introduced a novel feature aggregation method based on a multi-layer perceptron (MLP) from multiple feature maps, with a focus on improving per-query runtimes.

Many state-of-the-art VPR methods also introduce novel training and fine-tuning techniques for backbone feature extractors, improving image retrieval performance. CosPlace [4] redesigned VPR as an image classification problem, which circumvented slow training times often incurred for contrastive loss methods. CricaVPR [26] introduced an attention mechanism to correlate multiple images in a batch during training, significantly reducing training time whilst improving place matching accuracy. AP-GeM [35] developed an average precision loss function with a GeM pooling layer using advances in listwise loss functions and histogram binning approximations. CliqueMining [17] creates challenging batches of images for contrastive learning through generating graphs of similar looking places to maximize VPR performance in highly aliased scenarios.

B. Event-based localization

To date, there are several methods that have been developed for the purposes of performing VPR using event-based data. Almost all methods require event images to be constructed over either fixed time window or fixed event count, where the length of the time window or number of events for reconstruction can dramatically alter the performance of each system [15]. Methods that use event count histogram images are, typically, less accurate [15] due to the sparseness in the feature space, whereas RGB image reconstructions with methods such as E2VID [34] allow using state-of-the-art VPR systems.

EventVLAD [23] was introduced as a denoising network for event frames to generate NetVLAD features for VPR, and was one of the first histogram-based methods. Sparse-Event-VPR explored the amount of pixel-wise information needed to perform effective VPR, generating quality performance with as few as 25 pixels [9]. LENS deployed the first event-based VPR

pipeline onto neuromorphic hardware for direct, asynchronous inferencing with off-chip readouts [14]. Recently, Flash performed sub-millisecond VPR using active pixel selection [33].

For image reconstruction methods, the challenge for localization becomes a question of the quality of reconstructions rather than VPR method effectiveness. By having access to state-of-the-art vision transformers and VPR methods, high quality reconstructions will assist these methods in performing better quality image retrieval. Event-LAB [15] showed that between histogram and reconstruction based images, the latter performed significantly better by upwards of 50% by being able to use VPR techniques such as CosPlace [4], EigenPlaces [5], and MixVPR [1]. As explored in [19], histogram based localization techniques can be enhanced through the ensembling of multiple techniques, including image reconstruction-based methods.

C. Deep-Learning Networks for Event Cameras

Unlike conventional images, event-based frames do not have a wide variety of pre-trained networks to extract quality features for VPR. The lack of pre-trained networks and large-scale datasets to fine-tune performance for localization specific tasks is part of the reason why few localization methods exist for event-based data. Relevant to this work, the teacher-student model with RGB and event-frames as introduced by [40] provides one of the few vision transformer (ViT) architectures that can be used for a variety of downstream tasks. An extension of this work was used for dense prediction tasks [41].

Several deep-learning architectures using event-based data have been developed for a variety of computer vision tasks. For Simultaneous Localization And Mapping (SLAM), feature detection and tracking techniques have been introduced using deep-learning architectures through systems such as EKLT [12] and SILC [27] integrating event-based cameras for fast, free of motion-blur. Fully end-to-end SLAM systems with event cameras that include deep learning of 6DOF pose and re-localization have been developed using recurrent networks [30, 18].

Another common deep learning task using events is optical flow, with techniques such as Ev-FlowNet [44] developed to learn motion estimation through self-supervision methods. Patch-based techniques measure visual motion by leveraging the sparsity of event pixel activation to generate a sparse, non-redundant format for optical flow estimation [21]. Optical flow techniques have also been integrated into egomotion calculation from event streams using unsupervised learning [45, 42] and generative adversarial networks [25].

III. METHOD

This work makes use of three pre-existing networks to extract features from event images: (i) Event-camera Data Pre-training (ECDPT) [40] for initial place prediction through descriptor cosine similarity after GeM pooling [32], (ii) keypoint detection from multi-channel time surface (MCTS) representations via SuperEvent [6] for refinement of place matches

performed through RANSAC re-ranking of top- k initial place matches, and (iii) depth estimation from tencode images via Depth AnyEvent [2] for an optional subsequent further refinement through depth images and structural similarity index. We name our system EventGeM, with the optional depth re-ranking as EventGeM-D, for clarity. Below, we detail the methods used to develop our system.

A. Initial place prediction

Event streams are defined as a series of events e with standardized format of:

$$e = [x, y, t, p], \quad (1)$$

where x, y are the pixel coordinates, t is the timestamp, and p is the polarity.

We pick a fixed time window Δt over which we accumulate events to generate an image-like representation of places as a tensor \mathbb{I} for initial feature extraction:

$$\mathbb{I}_{x,y,p} = \sum_{i \in \mathcal{E}_{\Delta t}} \delta(x - x_i) \delta(y - y_i) \delta(p - p_i), \quad (2)$$

where i indexes events in the stream and $\mathcal{E}_{\Delta t}$ denotes the set of events whose timestamps fall within the accumulation window, $p \in \{0, 1\}$ is the channel index corresponding to the polarity, and δ is the Kronecker delta function, which equals 1 if the arguments match and 0 otherwise.

Feature extraction of \mathbb{I} from the ECDPT [40] backbone ViT produces a $[H, W, C]$ embedding \mathcal{X} :

$$\mathcal{X}_{[H,W,C]} = \mathbf{ViT}(\mathbb{I}_{x,y,c}), \quad (3)$$

where H, W is height and width and C is the number of output channels [40].

GeM pooling is commonly used for image matching techniques and provides a balance between average and max pooling over several channels to provide a compact descriptor for VPR [32] (Fig. 2). For a given \mathcal{X} , the output feature vector \mathbf{f} is calculated as:

$$\mathbf{f} = \left(\frac{1}{HW} \sum_{i=1}^H \sum_{j=1}^W (\mathcal{X}_{i,j,C})^\gamma \right)^{\frac{1}{\gamma}}, \quad (4)$$

where γ is a learnable parameter for GeM pooling.

We concatenate reference \mathbf{f}_{ref} and query \mathbf{f}_{qry} descriptors into descriptor matrices \mathbb{F} to compute the cosine similarity matrix \mathbb{C} :

$$\begin{aligned} \mathbb{F}_{\text{ref}} &= \left[\mathbf{f}_{\text{ref}}^{(1)} \mathbf{f}_{\text{ref}}^{(2)} \cdots \mathbf{f}_{\text{ref}}^{(N_r)} \right]^\top, \\ \mathbb{F}_{\text{qry}} &= \left[\mathbf{f}_{\text{qry}}^{(1)} \mathbf{f}_{\text{qry}}^{(2)} \cdots \mathbf{f}_{\text{qry}}^{(N_q)} \right]^\top, \\ \mathbb{C} &= \mathbb{F}_{\text{ref}} \mathbb{F}_{\text{qry}}^\top, \end{aligned} \quad (5)$$

where \top denotes the matrix transpose.

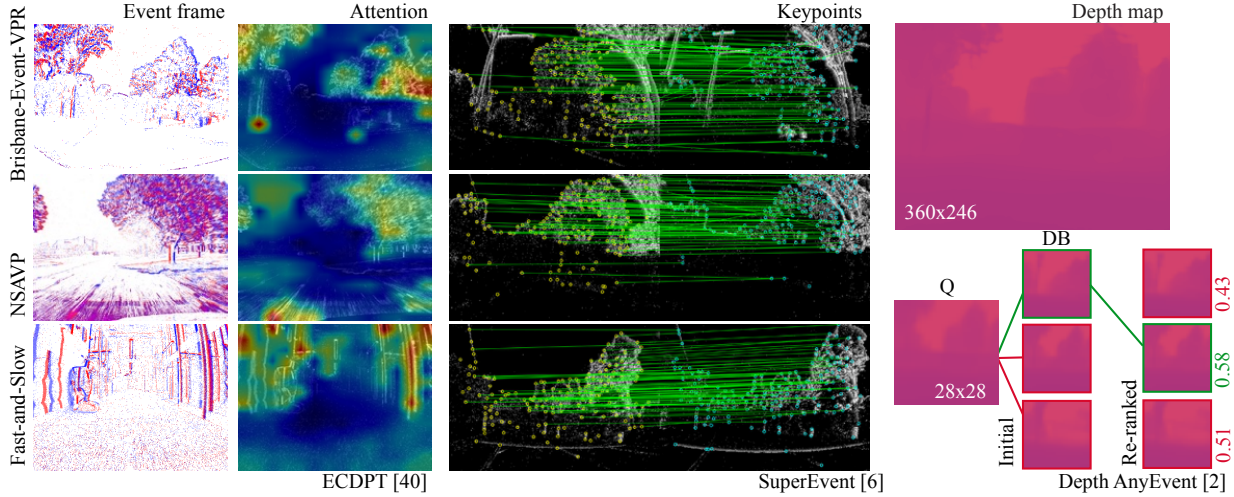


Fig. 2: Example event frames and attention maps generated after GeM pooling from the pre-trained ViT backbone [40] for the datasets used in this work—Brisbane-Event-VPR [8], NSAVP [7], and Fast-and-Slow [29]. Query and reference matches with keypoint descriptors used for 2D-homography based re-ranking with RANSAC. Example query and database matches using EventGeM-D from depth maps generated by Depth AnyEvent [2] using SSIM re-ranking after keypoint RANSAC, with the highest similarity score indicating a correct match.

For each query place $q \in \{1, \dots, N_q\}$, we denote its similarity vector as the q -th column of \mathbb{C} :

$$\mathbf{c}_q = \mathbb{C}(:, q). \quad (6)$$

We then select the top- k reference candidates:

$$\hat{\mathbf{p}}_k(q) = \{i_1, \dots, i_k\}, \quad \{i_1, \dots, i_k\} = \arg \text{top}_k(\mathbf{c}_q), \quad (7)$$

where $\{i_1, \dots, i_k\}$ are the indices of the k highest similarity scores in \mathbf{c}_q with $\hat{\mathbf{p}}_k(q)$ forming the shortlist passed to keypoint-based re-ranking.

B. Keypoint re-ranking

Keypoints are detected using SuperEvent SE on MCTS place representations [6]. We first construct MCTS representations \mathbb{M} from e . Given a set of time constants $\{\tau_1, \dots, \tau_K\}$, we construct the MCTS representation $\mathbb{M} \in \mathbb{R}^{H \times W \times 2 \times K}$ by computing the exponential decay of the time elapsed since the last event at each pixel (x, y) and polarity p :

$$\mathbb{M}_{x,y,p,k} = \exp\left(-\frac{t_{\text{ref}} - t_{\text{last}}(x, y, p)}{\tau_k}\right), \quad (8)$$

where t_{ref} is the current timestamp and $t_{\text{last}}(x, y, p)$ is the timestamp of the most recent event at that pixel and polarity. If no event occurred within the window, we set $\mathbb{M}_{x,y,p,k} = 0$.

We then extract keypoints and descriptors from references and queries:

$$KP^{qry}, D^{qry} = \mathbf{SE}(\mathbb{M}^{qry}), \quad (9)$$

$$KP^{ref}, D^{ref} = \mathbf{SE}(\mathbb{M}^{ref}), \quad (10)$$

where KP^{qry} and KP^{ref} are the detected 2D keypoint locations in the query and reference, respectively, and D^{qry}

and D^{ref} are the corresponding local descriptors. From these, we next compute a set of tentative descriptor matches \mathcal{M}_{QR} using the nearest-neighbour ratio (NNR) test:

$$\mathcal{M}_{QR} = \text{NNR}(D^{qry}, D^{ref}), \quad (11)$$

where each match in \mathcal{M}_{QR} associates a descriptor from D^{qry} to its corresponding descriptor in D^{ref} .

We estimate a homography \mathbf{H}_{QR} from these correspondences using RANSAC where the set of geometrically verified inliers \mathcal{I}_{QR} is:

$$\mathcal{I}_{QR} = \{(\mathbf{p}^Q, \mathbf{p}^R) \in \mathcal{M}_{QR} \mid \|\mathbf{p}^R - \pi(\mathbf{H}_{QR} \tilde{\mathbf{p}}^Q)\|_2 < \epsilon\}, \quad (12)$$

where $\tilde{\mathbf{p}} = [x, y, 1]^\top$ denotes homogeneous coordinates, $\pi(\cdot)$ converts homogeneous coordinates back to Euclidean coordinates, and ϵ is the RANSAC re-projection threshold.

For each query and shortlisted reference candidate $i \in \hat{\mathbf{p}}_k(q)$, we define a re-ranked similarity score by combining the global cosine similarity with the geometric inlier count:

$$s'_{q,i} = \mathbb{C}_{i,q} + \alpha |\mathcal{I}_{Q_q R_i}|, \quad (13)$$

where $|\mathcal{I}_{Q_q R_i}|$ is the number of RANSAC-verified inlier matches (Eq. 12) and α is a weighting hyper-parameter.

We then re-rank the initial shortlist $\hat{\mathbf{p}}_k(q)$ by selecting the candidates with the largest $s'_{q,i}$:

$$\hat{\mathbf{p}}_k^{\text{kp}}(q) = (i_1, \dots, i_k), \quad (i_1, \dots, i_k) = \arg \text{top}_k_{i \in \hat{\mathbf{p}}_k(q)}(s'_{q,i}), \quad (14)$$

C. Depth re-ranking

In EventGeM-D, we can further refine the re-ranked predictions from the keypoint based RANSAC for structural

similarity index metric (SSIM) comparison by computing a new top- k selection from the re-ranked query columns (Fig. 2).

For the depth estimation using Depth AnyEvent DAE [2], we generated Tencode \mathbb{T} representations that are similar to the polarity frames in Eq. 2 and include an additional channel that represents time. For a set of events e_i at a fixed time window $\Delta t = [t_{\min}, t_{\max}]$, $i_{x,y}^*$ is the index of the most recently active event at pixel x, y :

$$i_{x,y}^* = \max\{i \mid t_i \in \Delta t, x_i = x, y_i = y\}. \quad (15)$$

The temporal recency of $i_{x,y}^*$ is then defined as:

$$\tau_i = 1 - \frac{t_i - t_{\min}}{t_{\max} - t_{\min} + \varepsilon}. \quad (16)$$

With the final Tencode tensor $\mathbb{T}_{x,y,c}$ being calculated as:

$$\mathbb{T}_{x,y,c} = [p_{i^*}, \tau_i, 1 - p_{i^*}]. \quad (17)$$

We then retrieve the depth estimation maps \mathcal{D} from DAE:

$$\mathcal{D} = \text{DAE}(\mathbb{T}_{x,y,c}) \quad (18)$$

\mathcal{D} are then resized to a height and width of 28×28 before SSIM calculation, which produces a score from $[0, 1]$. Once SSIM scores $s_{q,i}^{\text{ssim}}$ have been computed for all candidates: $i \in \hat{\mathbf{p}}_k^{\text{kp}}(q)$, we re-rank the shortlist by sorting in descending order for the final place prediction rankings $\hat{\mathbf{p}}_k^{\text{ssim}}(q)$:

$$\hat{\mathbf{p}}_k^{\text{kp}}(q) = (i_1, \dots, i_k), \quad (i_1, \dots, i_k) = \text{argsort}_{i \in \hat{\mathbf{p}}_k(q)}(-s'_{q,i}) \quad (19)$$

IV. EXPERIMENTAL SETUP

Here, we detail the hyperparameters for GeM pooling and RANSAC re-ranking in Section IV-A, the baseline methods and datasets used in Section IV-B, the evaluation metrics in Section IV-C, and finally our implementation environment for EventGeM in Section IV-D.

A. Hyperparameters

To use the ECDPT backbone [40] for VPR, we integrated a GeM pooling layer for compact feature descriptor generation, which is traditionally a trainable component for image matching techniques to maximize performance based on the dataset type [32]. However, GeM training typically requires many images from large scale datasets with positive and negative samples. In event-based VPR, there exists no dataset that meet such criteria for the purposes of finetuning models. As such, we elected to use a fixed value for $\gamma = 5.0$ in the GeM pooling through trialling multiple values, maximizing for a higher Recall@K=1 (R@1) (Tab. IV).

For the RANSAC re-ranking we computed the feature matches from the top $k = 50$ places, with an $\epsilon = 5.0$ and an $\alpha = 0.05$.

B. Baseline Methods and Datasets

For all baseline method evaluation and datasets in this study, we used Event-LAB to generate event frames, run baseline methods, and obtain evaluation metrics [15]. There are limited event-based VPR methods, acknowledging that many conventional VPR systems work well with images reconstructed from event streams, such as from E2VID [34, 15]. In this work, we follow the baseline methods outlined in Event-LAB, specifically LENS [14], Sparse-Event-VPR [9], and Event-VLAD [23]. We also compare matches directly from the backbone ViT models ECDPT+GeM [35, 40], and SuperEvent [6] using the Brute-Force matcher from OpenCV to match keypoint descriptors. Finally, we compare our results to image reconstructions from E2VID [34] with the conventional VPR method AP-GeM [35], that also used a GeM pooling layer for image retrieval using a pre-trained backbone, Resnet101-AP-GeM.

We evaluate our method on the Brisbane-Event-VPR [8], NSAVP [7], and Fast-and-Slow [29] datasets. For each dataset, we performed all evaluations on a variety of query traverses under different conditions with a single reference, following precedence in the literature [4, 15]. The Brisbane-Event-VPR dataset was captured using a DAVIS346 event camera, with the Sunset2 traverse as the reference, and queried with Sunset1, Morning, and Night [8]. The NSAVP was captured using an iniVation DVXplorer, and we use R0-FA0 as reference traverse and R0-FS0 and R0-FN0 as query traverses [7]. Finally, we used the Fast-and-Slow dataset to evaluate the performance of all methods in an indoor environment using R-med1 as the reference and Q-high1, Q-med1, and Q-low1 as the references [29].

All event frame images (polarity histogram and tencode) for the main experiments were generated using a max t of 50 msec, with the MCTS representation using a range of reconstruction times [10, 20, 30, 40, 50] msec per time channel. 50 msec was chosen as Depth AnyEvent [2] was developed using this time window, acknowledging that other methods of generating event frames, such as through event counts per frame, provide benefits such as mitigating velocity differences between references and queries [15].

C. Evaluation metrics

The main evaluation metric we used in this study is the Recall@K, which measures if any of the Top K matches that a VPR system predicts falls within the ground truth. Formally, recall R is defined as:

$$R = \frac{TP}{GTP} \quad (20)$$

where TP is the number of true positive matches and GTP is the total number of possible ground truth positive matches. We measure and report the Recall@K = [1, 5, 10] (R@1, R@5, R@10).

We additionally investigated the per-query runtime, in Hz, including the generation of the necessary event frame representations, and running the respective VPR algorithm. For

all of our evaluations, we set a ground truth tolerance of 70 m to allow a predicted place to be within to be considered correctly matched for outdoor datasets [8, 7], and 3 m for indoor evaluation [29], following [9].

D. System environment

EventGeM is implemented in Python3 and Pixi [10]. Experiments were performed on an Ubuntu 24.04 desktop computer with an Nvidia 8GB RTX2080 graphics processor unit and a high-performance computing (HPC) cluster, using an Nvidia 40GB A100 GPU, for the computationally intensive methods. The on-robot demonstration used a Jetson Orin AGX 64GB Developer Kit running JetPack 6.2.

V. RESULTS

A. Recall performance of EventGeM

Here, we compare EventGeM to other event-based VPR methods for across a variety of datasets. Table I shows the Recall@K performance of our method and baselines using the Brisbane-Event-VPR [8] dataset. EventGeM and EventGeM-D was able to significantly outperform the best available event-based VPR method, EventVLAD, by 48% in absolute R@1. EventGeM and EventGeM-D displayed a consistent increase in performance across the varying challenging lighting conditions when comparing sunset, daytime, and morning conditions. A key highlight of both our methods is that we achieve high performance using small time windows of 50 msec, which produces on average 12,000 – 14,000 images per reference and query pair. For a fair comparison, we include the results of the baseline methods both with and without re-ranking using SuperEvent keypoints and RANSAC of the top- k matches from each method [6].

When using EventGeM and EventGeM-D with the NSAVP dataset [7], we achieve outperform the best performing event-frame baseline method by 40% (EventVLAD [23]) and 9% to E2VID+AP-GeM [35, 34], as summarized in Table II. However, when comparing a daytime and nighttime scenario, as is the case between R0-FA0 and R0-FN0, performance for EventGeM and all baselines is low at $\approx 10\%$ R@1. This is likely due to the lack of adaptively biasing of event-cameras for different lighting conditions, which remains a challenge for event datasets in VPR [29]. Across both the Brisbane-Event-VPR and NSAVP datasets, however, we observe that our re-ranking strategy is able to provide an increase in the Recall@K metrics above their respective baselines.

Finally, when comparing performance for an indoor dataset, Fast-and-Slow [29]. Fast-and-Slow is a dataset that was introduced that improves VPR dataset collection by adaptively biasing DVS for different lighting conditions to provide an optimal event rate [29]. The best performing method was AP-GeM with E2VID reconstructed images [34, 35], which achieved 100% accuracy in the Q-med1 and Q-high1 queries. EventGeM and EventGeM-D performed comparably at above 94% R@1 on average (Table III).

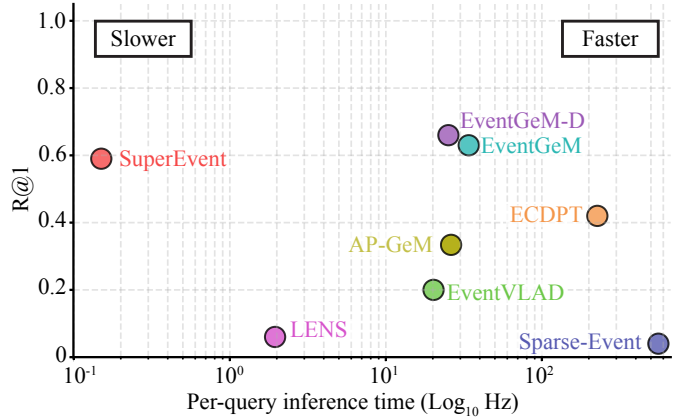


Fig. 3: EventGeM, EventGeM-D, and baseline method runtime per-query plotted against the average Recall@1 for the Brisbane-Event-VPR [8] dataset. Values are the average recall and runtime performance with Sunset2 as the reference against Sunset1, Morning, and Daytime.

B. Runtime performance

We next compared the per-query run time of each method, from the time taken to stream individual events from a file containing all events to running the processing algorithm to obtain a match (Fig. 3). Both EventGeM and EventGeM-D achieved real-time inference at 33.97 and 25.17 Hz, respectively (Fig. 3). The backbone elements of EventGeM, ECDPT [40] and SuperEvent [6], achieved a per-query inference time of 226.67 and 0.15 Hz, respectively (Fig. 3). SuperEvent was particularly slow due to the brute force matching technique of keypoint descriptors to 12,828 references, hence indicating the advantage of performing initial coarse predictions with global descriptors and re-ranking from a top- k [40, 6].

EventVLAD [23] ran with an average frequency of 20.21 Hz (Fig. 3). However, in comparison to EventVLAD, EventGeM and EventGeM-D performed with a significantly higher recall from an average of 0.2 R@1 to 0.63 and 0.66 R@1, respectively. LENS [14] and Sparse-Event-VPR [9] both performed similarly to each other in terms of absolute recall, however had vastly different runtime frequencies at 1.95 and 558 Hz, respectively (Fig. 3). The E2VID+AP-GeM method performed comparably to EventGeM with an average per-query runtime of 27.17 Hz [34, 35].

We do acknowledge, however, that reducing the reference database size through subsampling would improve runtime frequencies for methods like SuperEvent significantly. Overall, we establish that EventGeM finds the best balance across all baseline methods in terms of recall performance and per-query runtime – demonstrating state-of-the-art performance.

C. Online demonstration

Finally, to demonstrate the capability of our system to be used for real-world accurate event-based localization, we deployed the EventGeM model onto a robotic platform for

TABLE I: Recall@K performance of VPR baselines for Brisbane-Event-VPR with Sunset2 as the reference. **Bold** best performance. Underline is second best performance. \uparrow Higher values are better. Values next to reference and query names indicates number of places.

Method (Ref: Sunset2 - 12,828)	Sunset1 - 14,481			Morning - 13,456			Daytime - 14,321		
	R@1	R@5	R@10	R@1	R@5	R@10	R@1	R@5	R@10
LENS [14]	0.09	0.16	0.20	0.05	0.10	0.14	0.04	0.8	0.13
Sparse-Event-VPR [9]	0.05	0.08	0.13	0.02	0.04	0.05	0.05	0.08	0.09
EventVLAD [23]	0.43	0.57	0.64	0.09	0.17	0.22	0.08	0.16	0.22
LENS [14]+Re-rank	0.19	0.22	0.24	0.12	0.15	0.18	0.09	0.12	0.16
Sparse-Event-VPR [9]+Re-rank	0.11	0.12	0.15	0.03	0.04	0.05	0.05	0.09	0.10
EventVLAD [23]+Re-rank	0.68	0.72	0.74	0.21	0.25	0.28	0.19	0.24	0.28
E2VID+AP-GeM [34, 35]	0.59	0.71	0.76	0.24	0.32	0.36	0.13	0.22	0.27
ECDPT+GeM [40]	0.77	0.86	0.90	0.29	0.48	0.58	0.19	0.36	0.45
SuperEvent [6]	0.86	0.89	0.90	0.53	<u>0.67</u>	0.73	0.37	<u>0.51</u>	0.59
EventGeM (ours)	<u>0.90</u>	<u>0.92</u>	<u>0.93</u>	0.60	0.66	<u>0.69</u>	<u>0.39</u>	0.47	<u>0.52</u>
EventGeM-D (ours)	0.91	0.93	0.94	0.63	0.70	0.73	0.45	0.54	0.59

TABLE II: Recall@K performance of VPR baselines for NSAVP with R0-FA0 as the reference. **Bold** best performance. Underline is second best performance. \uparrow Higher values are better. Values next to reference and query names indicates number of places.

Method (Ref: R0-FA0 (20,957))	R0-FS0 (18,218)			R0-FN0 (17,793)		
	R@1	R@5	R@10	R@1	R@5	R@10
LENS [14]	0.17	0.24	0.30	0.03	0.08	0.11
Sparse-Event-VPR [9]	0.14	0.24	0.29	0.02	0.08	0.11
EventVLAD [23]	0.20	0.28	0.33	0.05	0.11	0.14
LENS [14]+Re-rank	0.27	0.32	0.35	0.04	0.08	0.12
Sparse-Event-VPR [9]+Re-rank	0.19	0.27	0.31	0.04	0.08	0.11
EventVLAD [23]+Re-rank	0.34	0.38	0.40	0.05	0.10	0.13
E2VID+AP-GeM [34, 35]	0.51	0.60	0.64	0.06	0.10	0.12
ECDPT+GeM [40]	0.36	0.50	0.57	0.05	0.11	0.15
SuperEvent [6]	0.34	0.46	0.51	0.05	0.12	0.17
EventGeM (ours)	<u>0.59</u>	<u>0.64</u>	<u>0.66</u>	<u>0.10</u>	<u>0.18</u>	<u>0.22</u>
EventGeM-D (ours)	0.60	0.66	0.68	0.11	0.20	0.23

online VPR (Fig. 4). We mounted an iniVation DAVIS346 event camera and a Jetson Orin AGX 64GB Developer Kit to an Agile Scout Mini robot to perform real-time, on-robot localization. In order for EventGeM to run on the robotic platform, we used the popular ONNX ecosystem to compile both the ECDPT [40] backbone and SuperEvent model [6] directly onto the Jetson.

When testing on an indoor environment, we are able to demonstrate high-accuracy localization achieving an R@1 of 0.88 with the distance matrix following closely to the ground truth (Fig. 4). We achieved an average runtime of ≈ 24 Hz per query, with the majority of queries above 20 Hz (Fig. 4). The high accuracy and appropriate run-times for EventGeM to provide edge capable localization demonstrate the potential for the integration of event-based cameras in robotics applications.

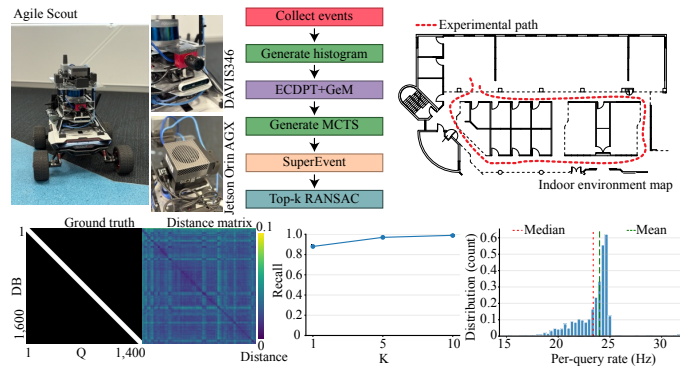


Fig. 4: Online deployment of EventGeM for real-time localization on a robotic platform. We used an Agile Scout 4-wheeled robot fitted with a DAVIS346 DVS and a Jetson Orin AGX running EventGeM. Events were collected over a 50 msec time window and processed by EventGeM, including the generation of the different representations for the ECDPT+GeM [40] backbone and the SuperEvent [6] keypoint detector. The robot was teleoperated around an indoor environment to capture a reference dataset and a query following the same experimental path. Our results show a strong alignment with the ground truth position, achieving a R@1 over 88% and an average runtime of 24 Hz per query.

D. Ablation Studies

Finally, we describe the ablation studies performed for EventGeM. Since we were not able to effectively train a GeM pooling layer, we evaluated how different values for the learnable parameter γ affected recall performance (Table IV). We find that $\gamma = 5.0$ works well at pooling the features from the EDCPT [40] backbone, with minimal differences in recall value across values from 1.0 to 10.0. A $\gamma = 1.0$ (which is operationally equivalent to an average pool) performs the worst overall (Table IV). The effects of γ on EventGeM and EventGeM-D was negligible, as the re-ranking strategies

TABLE III: Recall@K performance of VPR baselines for Fast-and-Slow with R-med1 as the reference. **Bold** best performance. Underline is second best performance. \uparrow Higher values are better. Values next to reference and query names indicates number of places.

Method (Ref: R-med1 - 1,272)	Q-low1 - 1,310			Q-med1 - 1,276			Q-high1 - 1,293		
	R@1	R@5	R@10	R@1	R@5	R@10	R@1	R@5	R@10
LENS [14]	0.16	0.25	0.32	0.20	0.32	0.39	0.28	0.38	0.42
Sparse-Event-VPR [9]	0.32	0.38	0.41	0.33	0.38	0.40	0.36	0.39	0.41
EventVLAD [23]	0.45	0.69	0.79	0.75	0.85	0.89	0.84	0.92	0.94
LENS [14]+Re-rank	0.27	0.34	0.38	0.33	0.40	0.45	0.38	0.44	0.46
Sparse-Event-VPR [9]+Re-rank	0.36	0.40	0.42	0.36	0.42	0.44	0.40	0.47	0.50
EventVLAD [23]+Re-rank	0.84	0.86	0.87	0.90	0.92	0.92	0.94	0.96	0.98
E2VID+AP-GeM [34, 35]	0.95	0.97	0.98	1.0	1.0	1.0	0.99	1.0	1.0
ECDPT+GeM [40]	0.77	0.89	0.92	0.91	0.94	<u>0.95</u>	0.94	0.95	0.96
SuperEvent [6]	0.93	<u>0.95</u>	<u>0.95</u>	0.94	0.94	<u>0.95</u>	<u>0.95</u>	<u>0.97</u>	<u>0.98</u>
EventGeM (ours)	<u>0.94</u>	0.94	0.94	0.94	<u>0.95</u>	<u>0.95</u>	<u>0.95</u>	<u>0.97</u>	<u>0.98</u>
EventGeM-D (ours)	0.93	0.94	0.94	<u>0.95</u>	<u>0.95</u>	<u>0.95</u>	<u>0.95</u>	<u>0.97</u>	<u>0.98</u>

TABLE IV: Effects of γ on GeM pooling and Recall@K performance for the Brisbane-Event-VPR [8] dataset. Reference dataset was Sunset2 and query was Sunset1.

γ	ECDPT+GeM [40]			EventGeM			EventGeM-D		
	R@1	R@5	R@10	R@1	R@5	R@10	R@1	R@5	R@10
1.0	0.72	0.84	0.88	0.89	0.91	0.92	0.90	0.92	0.93
2.5	0.74	0.85	0.89	0.89	0.91	0.92	0.90	0.92	0.93
5.0	0.77	0.86	0.86	0.90	0.92	0.93	0.91	0.93	0.94
7.5	0.77	0.87	0.90	0.91	0.92	0.93	0.91	0.93	0.94
10.0	0.77	0.87	0.90	0.91	0.92	0.93	0.91	0.93	0.94

TABLE V: Event image reconstruction time window (in msec) and Recall@K performance for the Brisbane-Event-VPR [8] Reference dataset was Sunset2 and query was Sunset1.

Δt (msec)	EventGeM			EventGeM-D		
	R@1	R@5	R@10	R@1	R@5	R@10
10	0.85	0.87	0.88	0.85	0.88	0.89
50	0.90	0.92	0.93	0.91	0.93	0.94
100	0.91	0.93	0.94	0.92	0.95	0.96
250	0.90	0.92	0.93	0.90	0.94	0.95

overcame any minor differences in top- k prediction retrievals.

We additionally explored to what extent the event reconstruction time window changed performance (Table V). The selected time window of 50 msec for the main experiments proved to perform comparably, with little variation in recall at longer time windows, with a slight degradation in performance at 10 msec. The re-ranking with keypoints was not further enhanced by the optional depth based re-rank time windows other than 50 msec, likely indicating that the Depth AnyEvent predictions are tuned to work only at that time window [2].

VI. CONCLUSION

In this work, we present EventGeM, a state-of-the-art event-based VPR system that leverages pre-trained vision transformers and keypoint detectors to perform accurate localization. We found that across multiple datasets and conditions, EventGeM consistently performed the most accurate localization when compared to several baseline methods. Importantly, we demonstrate EventGeM as a real-world capable solution to perform event-based VPR by deploying our pipeline end-to-end on a robotic platform, inferencing directly from event streams. This work represents a step forward in using event-based cameras for effective VPR.

We acknowledge certain limitations in the design and application of EventGeM and briefly discuss them here. First, we were unable to train the γ value for our GeM pooling layer due to the lack of effective VPR datasets with positive and negative pairs that can be found in datasets like Pittsburgh 30k [38] and Tokyo 24/7 [39]. This is a commonly encountered problem in the event-camera and event-vision community, highlighting a growing need for more datasets and benchmarking systems as the field grows. The second issue we acknowledge is the added complexity of mixing multiple event-based representations of the same place to perform the initial feature extraction [40] and the keypoint selection [6], which adds computational load and time. Finally, we additionally acknowledge the stark lack of VPR baseline methods to compare with. Although the event-based localization field is growing [23, 9, 14, 15], these methods are often designed for specific purposes that only just fit within the scope for comparison.

Overall, EventGeM represents a step forward in the performance of what is achievable with event cameras for localization systems and performs state-of-the-art VPR.

REFERENCES

- [1] Amar Ali-bey, Brahim Chaib-draa, and Philippe Giguère. MixVPR: Feature mixing for visual place recognition. In

- IEEE/CVF Winter Conference on Applications of Computer Vision*, pages 2998–3007, 2023.
- [2] Luca Bartolomei, Enrico Mannocci, Fabio Tosi, Matteo Poggi, and Stefano Mattoccia. Depth anyevent: A cross-modal distillation paradigm for event-based monocular depth estimation. In *Proceedings of the IEEE/CVF International Conference on Computer Vision (ICCV)*, October 2025.
 - [3] Gabriele Berton and Carlo Masone. Megaloc: One retrieval to place them all. In *Proceedings of the IEEE/CVF Conference on Computer Vision and Pattern Recognition (CVPR) Workshops*, pages 2861–2867, June 2025.
 - [4] Gabriele Berton, Carlo Masone, and Barbara Caputo. Rethinking visual geo-localization for large-scale applications. In *IEEE/CVF Conference on Computer Vision and Pattern Recognition*, pages 4878–4888, 2022.
 - [5] Gabriele Berton, Gabriele Trivigno, Barbara Caputo, and Carlo Masone. Eigenplaces: Training viewpoint robust models for visual place recognition. In *IEEE/CVF International Conference on Computer Vision*, pages 11080–11090, 2023. doi: 10.1109/ICCV51070.2023.01017.
 - [6] Yannick Burkhardt, Simon Schaefer, and Stefan Leutenegger. Superevent: Cross-modal learning of event-based keypoint detection for slam. In *Proceedings of the IEEE/CVF International Conference on Computer Vision (ICCV)*, pages 8918–8928, October 2025.
 - [7] Spencer Carmichael, Austin Buchan, Mani Ramanagopal, Radhika Ravi, Ram Vasudevan, and Katherine A Skinner. Dataset and benchmark: Novel sensors for autonomous vehicle perception. *Int. J. Rob. Res.*, 44(3):355–365, 2025. ISSN 0278-3649. doi: 10.1177/02783649241273554.
 - [8] Tobias Fischer and Michael Milford. Event-based visual place recognition with ensembles of temporal windows. *IEEE Robotics and Automation Letters*, 5(4):6924–6931, 2020.
 - [9] Tobias Fischer and Michael Milford. How many events do you need? event-based visual place recognition using sparse but varying pixels. *IEEE Robotics and Automation Letters*, 7(4):12275–12282, 2022. doi: 10.1109/LRA.2022.3216226.
 - [10] Tobias Fischer, Wolf Vollprecht, Bas Zalmstra, Ruben Arts, Tim de Jager, Alejandro Fontan, Adam D Hines, Michael Milford, Silvio Traversaro, Daniel Claes, and Scarlett Raine. Pixi: Unified software development and distribution for robotics and ai, 2025. URL <https://arxiv.org/abs/2511.04827>.
 - [11] G. Gallego, T. Delbruck, G. Orchard, C. Bartolozzi, B. Taba, A. Censi, S. Leutenegger, A. J. Davison, J. Conradt, K. Daniilidis, and D. Scaramuzza. Event-based vision: A survey. *IEEE Transactions on Pattern Analysis & Machine Intelligence*, 44(01):154–180, 2022. doi: 10.1109/TPAMI.2020.3008413.
 - [12] Daniel Gehrig, Henri Rebecq, Guillermo Gallego, and Davide Scaramuzza. Eklt: Asynchronous photometric feature tracking using events and frames. *International Journal of Computer Vision*, 128(3):601–618, Mar 2020. ISSN 1573-1405. doi: 10.1007/s11263-019-01209-w.
 - [13] Kaiming He, Xiangyu Zhang, Shaoqing Ren, and Jian Sun. Deep residual learning for image recognition, 2015. URL <https://arxiv.org/abs/1512.03385>.
 - [14] Adam D. Hines, Michael Milford, and Tobias Fischer. A compact neuromorphic system for ultra-energy-efficient, on-device robot localization. *Science Robotics*, 10(103):eads3968, 2025. doi: 10.1126/scirobotics.ads3968.
 - [15] Adam D. Hines, Alejandro Fontan, Michael Milford, and Tobias Fischer. Event-lab: Towards standardized evaluation of neuromorphic localization methods. In *Proceedings of the IEEE Conference on Robotics and Automation (ICRA)*, 2026.
 - [16] Sergio Izquierdo and Javier Civera. Optimal transport aggregation for visual place recognition. In *Proceedings of the IEEE/CVF Conference on Computer Vision and Pattern Recognition (CVPR)*, June 2024.
 - [17] Sergio Izquierdo and Javier Civera. Close, but not there: Boosting geographic distance sensitivity in visual place recognition. In *Computer Vision – ECCV 2024*, page 240–257, Berlin, Heidelberg, 2024. Springer-Verlag. ISBN 978-3-031-73463-2. doi: 10.1007/978-3-031-73464-9_15.
 - [18] Yifan Jin, Lei Yu, Guangqiang Li, and Shumin Fei. A 6-dofs event-based camera relocalization system by cnn-lstm and image denoising. *Expert Systems with Applications*, 170:114535, 2021. ISSN 0957-4174. doi: <https://doi.org/10.1016/j.eswa.2020.114535>.
 - [19] Therese Joseph, Tobias Fischer, and Michael Milford. Ensemble-based event camera place recognition under varying illumination. *IEEE Robotics and Automation Letters*, 2025. doi: 10.1109/LRA.2025.3641119.
 - [20] Nikhil Keetha, Avneesh Mishra, Jay Karhade, Krishna Murthy Jatavallabhula, Sebastian Scherer, Madhava Krishna, and Sourav Garg. Anyloc: Towards universal visual place recognition. *IEEE Robotics and Automation Letters*, 9(2):1286–1293, 2023. doi: 10.1109/LRA.2023.3343602.
 - [21] Daniel R. Kepple, Daewon Lee, Colin Prepsius, Volkan Isler, Il Memming Park, and Daniel D. Lee. Jointly learning visual motion and confidence from local patches in event cameras. In Andrea Vedaldi, Horst Bischof, Thomas Brox, and Jan-Michael Frahm, editors, *Computer Vision – ECCV 2020*, pages 500–516, Cham, 2020. Springer International Publishing. ISBN 978-3-030-58539-6.
 - [22] Delei Kong, Zheng Fang, Kuanxu Hou, Haojia Li, Junjie Jiang, Sonya Coleman, and Dermot Kerr. Event-VPR: End-to-end weakly supervised deep network architecture for visual place recognition using event-based vision sensor. *IEEE Transactions on Instrumentation and Measurement*, 71:1–18, 2022. doi: 10.1109/TIM.2022.3168892.
 - [23] Alex Junho Lee and Ayoung Kim. Eventvlad: Visual place recognition with reconstructed edges from event cameras. In *2021 IEEE/RSJ International Conference on Intelligent Robots and Systems (IROS)*, pages 2247–2252, 2021. doi: 10.1109/IROS51168.2021.9635907.
 - [24] Hyeongi Lee and Hyoseok Hwang. Ev-ReconNet: Visual place recognition using event camera with spiking neural networks. *IEEE Sensors Journal*, 23(17):20390–20399, 2023. doi: 10.1109/JSEN.2023.3298828.
 - [25] Xiuhong Lin, Chenhui Yang, Xuesheng Bian, Weiyan Liu, and Cheng Wang. Eagan: Event-based attention generative adversarial networks for optical flow and depth estimation. *IET Computer Vision*, 16(7):581–595, 2022. doi: <https://doi.org/10.1049/cvi2.12115>.
 - [26] Feng Lu, Xiangyuan Lan, Lijun Zhang, Dongmei Jiang, Yaowei Wang, and Chun Yuan. Cricavpr: Cross-image correlation-aware representation learning for visual place recognition. In *Proceedings of the IEEE/CVF Conference on Computer Vision and Pattern Recognition (CVPR)*, June 2024.
 - [27] Jacques Manderscheid, Amos Sironi, Nicolas Bourdis, Davide Migliore, and Vincent Lepetit. Speed invariant time surface for learning to detect corner points with event-based cameras. In *2019 IEEE/CVF Conference on Computer Vision and Pattern Recognition (CVPR)*, pages 10237–10246, 2019. doi: 10.1109/CVPR.2019.01049.
 - [28] Carlo Masone and Barbara Caputo. A survey on deep visual place recognition. *IEEE Access*, 9:19516–19547, 2021. doi: 10.1109/ACCESS.2021.3054937.
 - [29] Gokul B. Nair, Michael Milford, and Tobias Fischer. Enhancing visual place recognition via fast and slow adaptive biasing in event cameras. In *2024 IEEE/RSJ International Conference on Intelligent Robots and Systems (IROS)*, pages 3356–3363, 2024. doi: 10.1109/IROS58592.2024.10802384.
 - [30] Anh Nguyen, Thanh-Toan Do, Darwin G. Caldwell, and Nikos G. Tsagarakis. Real-time 6dof pose relocalization for

- event cameras with stacked spatial lstm networks. In *2019 IEEE/CVF Conference on Computer Vision and Pattern Recognition Workshops (CVPRW)*, pages 1638–1645, 2019. doi: 10.1109/CVPRW.2019.00207.
- [31] Maxime Oquab, Timothée Darcet, Théo Moutakanni, Huy Vo, Marc Szafraniec, Vasil Khalidov, Pierre Fernandez, Daniel Haziza, Francisco Massa, Alaaeldin El-Nouby, Mahmoud Assran, Nicolas Ballas, Wojciech Galuba, Russell Howes, Po-Yao Huang, Shang-Wen Li, Ishan Misra, Michael Rabbat, Vasu Sharma, Gabriel Synnaeve, Hu Xu, Hervé Jegou, Julien Mairal, Patrick Labatut, Armand Joulin, and Piotr Bojanowski. Dinov2: Learning robust visual features without supervision, 2024. URL <https://arxiv.org/abs/2304.07193>.
- [32] Filip Radenović, Giorgos Tolias, and Ondřej Chum. Fine-tuning cnn image retrieval with no human annotation, 2018. URL <https://arxiv.org/abs/1711.02512>.
- [33] Vignesh Ramanathan, Michael Milford, and Tobias Fischer. Prepare for warp speed: Sub-millisecond visual place recognition using event cameras. In *Proceedings of the IEEE Conference on Robotics and Automation (ICRA)*, 2026.
- [34] Henri Rebecq, René Ranftl, Vladlen Koltun, and Davide Scaramuzza. Events-to-video: Bringing modern computer vision to event cameras. *IEEE Conf. Comput. Vis. Pattern Recog. (CVPR)*, 2019.
- [35] Jerome Revaud, Jon Almazan, Rafael S. Rezende, and Cesar Roberto de Souza. Learning with average precision: Training image retrieval with a listwise loss. In *Proceedings of the IEEE/CVF International Conference on Computer Vision (ICCV)*, October 2019.
- [36] Stefan Schubert, Peer Neubert, Sourav Garg, Michael Milford, and Tobias Fischer. Visual place recognition: A tutorial. *IEEE Robotics & Automation Magazine*, 2024. doi: 10.1109/MRA.2023.3310859.
- [37] Karen Simonyan and Andrew Zisserman. Very deep convolutional networks for large-scale image recognition, 2015. URL <https://arxiv.org/abs/1409.1556>.
- [38] Akihiko Torii, Josef Sivic, Tomas Pajdla, and Masatoshi Okutomi. Visual place recognition with repetitive structures. In *Proceedings of the IEEE Conference on Computer Vision and Pattern Recognition (CVPR)*, June 2013.
- [39] Akihiko Torii, Relja Arandjelovic, Josef Sivic, Masatoshi Okutomi, and Tomas Pajdla. 24/7 place recognition by view synthesis. In *Proceedings of the IEEE Conference on Computer Vision and Pattern Recognition (CVPR)*, June 2015.
- [40] Yan Yang, Liyuan Pan, and Liu Liu. Event camera data pre-training. In *Proceedings of the IEEE/CVF International Conference on Computer Vision (ICCV)*, pages 10699–10709, October 2023.
- [41] Yan Yang, Liyuan Pan, and Liu Liu. Event camera data dense pre-training. In Aleš Leonardis, Elisa Ricci, Stefan Roth, Olga Russakovsky, Torsten Sattler, and Gül Varol, editors, *Computer Vision – ECCV 2024*, pages 292–310, Cham, 2025.
- [42] Chengxi Ye, Anton Mitrokhin, Cornelia Fermüller, James A. Yorke, and Yiannis Aloimonos. Unsupervised learning of dense optical flow, depth and egomotion with event-based sensors. In *2020 IEEE/RSJ International Conference on Intelligent Robots and Systems (IROS)*, pages 5831–5838, 2020. doi: 10.1109/IROS45743.2020.9341224.
- [43] Xiwu Zhang, Lei Wang, and Yan Su. Visual place recognition: A survey from deep learning perspective. *Pattern Recognition*, 113:107760, 2021. doi: <https://doi.org/10.1016/j.patcog.2020.107760>.
- [44] Alex Zhu, Liangzhe Yuan, Kenneth Chaney, and Kostas Daniilidis. Ev-flownet: Self-supervised optical flow estimation for event-based cameras. In *Proceedings of Robotics: Science and Systems*, Pittsburgh, Pennsylvania, June 2018. doi: 10.15607/RSS.2018.XIV.062.
- [45] Alex Zihao Zhu, Liangzhe Yuan, Kenneth Chaney, and Kostas Daniilidis. Live demonstration: Unsupervised event-based learning of optical flow, depth and egomotion. In *2019 IEEE/CVF Conference on Computer Vision and Pattern Recognition Workshops (CVPRW)*, pages 1694–1694, 2019. doi: 10.1109/CVPRW.2019.00216.